submitted to J. Eur. Ceram. Soc. in Sept. 2002

First-Principles Calculations of the Dielectric Properties of Perovskite-type Materials

Eric Cockayne[1]

[1] *Ceramics Division, Materials Science and Engineering Laboratory, National Institute of Standards and Technology Gaithersburg, Maryland 20899-8520 USA*

Abstract

We compare first-principles (FP) calculations of the ionic effective charges, phonon frequencies, and static dielectric permittivities κ_s of several perovskite-type materials. Transition metal ions have anomalously large effective charges, though in the double perovskite $CaAl_{1/2}Nb_{1/2}O_3$ (CAN), the effective charge of Nb is significantly lower than in the simple perovskite $KNbO_3$, showing different Nb-O bonding chemistry. Tolerance factors, cation chemistry, and structural phase transitions all affect the nature of the softest phonons in perovskites. For the solid solution $(CaAl_{1/2}Nb_{1/2}O_3)_{1-x}$-$(CaTiO_3)_x$ (CAN-CT), κ_s is modeled via a cluster expansion, with the parameters determined from FP. In pure CAN, κ_s is found to increase when cation disorder increases, in agreement with experimental results on analogous systems. The dielectric constant of CAN-CT increases nonlinearly with x, in agreement with experiment.

KEYWORDS: dielectric properties; perovskites; first-principles calculations

PACS numbers: 77.22.Ch, 77.84.Dy, 63.20.Dj

I. INTRODUCTION

Dielectric materials for microwave applications must have high permittivity, low loss, and temperature stability. Uncovering the relationship between structure, chemistry, and dielectric properties is important for the eventual rational design of new dielectric materials.

Dispersion theory[1–3] provides a bridge between the crystal structure and chemistry and the dielectric properties. The static dielectric constant of a ceramic, κ_s, taken as the directional average of the dielectric tensor, is

$$\kappa_s = \kappa_\infty + \sum_\mu \kappa_\mu, \tag{1}$$

where κ_∞ is the directional average of the electronic dielectric tensor and κ_μ is the oscillator strength of mode μ. κ_μ, in turn is given by (SI units):

$$\kappa_\mu = \sum_{\alpha i \gamma j \delta} \frac{Z^\star_{i\alpha\gamma} Z^\star_{j\alpha\delta} (a_\mu)_{i\gamma} (a_\mu)_{j\delta}}{12\pi^2 m_i^{1/2} m_j^{1/2} V \epsilon_0 \nu_\mu^2}, \tag{2}$$

where i and j label ions, $\overleftrightarrow{Z}^\star_i$ is the Born effective charge tensor for ion i, ν_μ is the frequency for mode μ, and a_μ is the normalized dynamical matrix eigenvector for mode μ. The number of modes in Eq. (1) is determined by the crystal structure, whereas the values of $\overleftrightarrow{Z}^\star_i$, a_μ and ν_μ in Eq. (2) are determined by the crystal chemistry.

Ordered perovskite-type materials typically have around 20 atoms per unit cell. The quantities $\overleftrightarrow{Z}^\star_i$ and a_μ are difficult to determine experimentally for such systems. First principles (FP) calculations are ideally suited for studying periodic systems of this size and furthermore allow all of the quantities in Eqs. (1)-(2) to be determined.

The frequency dependent dielectric constant is given by complex $\kappa(\nu) = \kappa'(\nu) + i\kappa''(\nu)$. In materials of interest for microwave applications, however, κ' does not vary significantly between zero frequency and microwave frequencies. In this work, we neglect dielectric loss and frequency dependence of κ' and focus on κ_s as given by Eqs. (1)-(2).

To better understand structure-dielectric property relationships in microwave dielectric materials, we review in this work FP studies of the phonon and dielectric properties of simple perovskite-type materials, and extend FP studies to larger systems via a cluster expansion method.

II. METHODS

In order to compute κ_s, one must compute κ_∞, ν_μ, a_μ, and $\overleftrightarrow{Z}^\star_i$. All of these quantities can be calculate from density functional theory. The phonon frequencies and eigenvectors come from the dynamical matrix, which is determined by the force constant matrix $F_{i\alpha j\beta}$. Two different approaches exist for computing κ_∞, $\overleftrightarrow{Z}^\star_i$, and $F_{i\alpha j\beta}$, all of which are response quantities. The first is finite difference methods[3]. Finite difference methods have the advantage of easy implementation. The second is linear response, based on density functional perturbation theory[4–6]. This approach, though more difficult to implement, has the advantage of allowing perturbations of wavelength larger than the unit cell of the system to be studied.

For full details on the FP calculations reported in this work, refer to the original articles cited in the tables. For the results presented here that are not otherwise cited, the density functional theory package VASP was used[7–10], in conjunction with finite difference methods[3, 11]. VASP uses a plane wave basis set for the electronic wavefunctions, and ultrasoft Vanderbilt-type pseudopotentials[12] for the ions, as supplied by G. Kresse and J. Hafner[13]. We included semicore electrons for all metal ions. The plane-wave energy cutoff was 457.4 eV. The local density approximation (LDA) was used for the exchange-correlation energy. Brillouin zone integration was obtained by calculating Kohn-Sham wavefunctions for a grid equivalent to an $8 \times 8 \times 8$ Monkhorst-Pack grid for a primitive perovskite cell.

III. RESULTS

A Perovskites with small unit cells

Results for the effective charges, phonon properties, and dielectric properties for several perovskite systems of microwave interest are given in Tables I-III, along with results for some other perovskites. In order to simplify presentation and comparison, the Born effective charge tensors were reduced as follows:

$$Z^\star_s = \pm\Big(\frac{1}{3N_s}\sum_{i\in s}\sum_{\alpha\beta}(Z^\star_{i\alpha\beta})^2\Big)^{1/2}, \tag{3}$$

for species s, where the + sign is for cations and the − sign for anions. Oxygen ions have highly anisotropic Born effective charge tensors, thus we define the effective charge of O in the direction of the B cation, $Z^\star_{O,\parallel}$, and the effective charge of O transverse to the B cation, $Z^\star_{O,\perp}$, as follows:

$$Z^\star_{O,\parallel} = -\Big(\frac{1}{N_O}\sum_\alpha \sum_{i\in O_\alpha} \sum_\beta (Z^\star_{i\alpha\beta})^2\Big)^{1/2} \tag{4}$$

and

$$Z^\star_{O,\perp} = -\Big(\frac{3}{2}Z^\star_O - \frac{1}{2}Z^\star_{O,\parallel}\Big), \tag{5}$$

where O_α is an oxygen ion whose nearest neighbor B cations are in the $\pm\hat{\alpha}$ Cartesian directions. In the case where the perovskite is simple with Pm3m symmetry, or double with Fm3m symmetry, the $\overleftrightarrow{Z}^\star_i$ are diagonal and the components listed in Table I are exactly the diagonal components of $\overleftrightarrow{Z}^\star_i$.

For a cubic ABO_3 perovskite, there are three polar phonon triplets: a Last mode (A vibrates against B and O) a Slater mode (B vibrates against O), and an "O_6 bending" mode ($O_\parallel$ vibrates against $O_\perp$), Some mixing among these modes may occur. For a cubic double perovskite $AB_{1/2}B'_{1/2}O_3$, a fourth polar triplet exists where B and B′ vibrate against each other. When the cubic symmetry is broken, however, through ferroelectric distortion or octahedral tilting, the number of distinct polar modes typically increases. To facilitate comparison, results for distorted perovskites are grouped into the appropriate number of pseudotriplets, as discussed in Ref. [11].

Since the first-principles results for κ_s are based on FP ground state structures, it is appropriate to compare them with experiments at low temperature. The computed κ_s for $CaTiO_3$ agrees well with the experimental results at 4 K (Ref. [14]). Assuming that τ_f for $CaAl_{1/2}Nb_{1/2}O_3$ is temperature-independent, it can be inferred from Ref. [24] that its κ_s is about 24.5 at T = 0, in excellent agreement with the computed value. $BaTiO_3$ is ferroelectric and has strong temperature dependence of κ_s down to low temperatures[15], making comparison with experiment difficult.

B Disordered perovskites and Solid Solutions

It is not possible to compute the dielectric properties of disordered solids, partially ordered solids, or solid solutions directly from FP at present, because any periodic cell large enough to be representative of the disorder will be too computationally expensive. Many systems of microwave interest, however, are based on solid solutions. In particular, if a complete solid solution series exists between a material with positive τ_f and one with negative τ_f then it contains one or more compositions where $\tau_f = 0$. For example, $(CaAl_{1/2}Nb_{1/2}O_3)_{1-x}$-$(CaTiO_3)_x$ (CAN-CT) has $\tau_f = -88\ \mu K^{-1}$ at $x = 0$, $\tau_f = +712\ \mu K^{-1}$ at $x = 1$ and $\tau_f = 0$ at $x \approx 0.5$ [24].

Large supercells of CAN-CT were studied using cluster expansion methods. The cation species at site i was given the spinlike variable σ_i, with values -1, 0, and 1 corresponding to Al, Ti, and Nb, respectively. The total energy was expanded in the usual manner

$$E = E_0 + \sum_i \sum_{n=1}^{2} E_{1n}\sigma_i^n + \sum_{i,\mathbf{R}} \sum_{m,n=1}^{2} E_{2\mathbf{R}mn}\sigma_i^m\sigma_{i+\mathbf{R}}^n + \dots . \tag{6}$$

The Born effective charges were likewise expanded:

$$Z^\star_{i\alpha\beta} = Z^\star_{i\alpha\beta 0} + \sum_j \sum_{n=1}^{2} Z^\star_{i\alpha\beta 1jn}\sigma_j^n + \sum_{jk} \sum_{m,n=1}^{2} Z^\star_{i\alpha\beta 2jkmn}\sigma_j^m\sigma_k^n + \dots \tag{7}$$

The force constant matrix and κ_∞ were expanded in a similar fashion.

Each symmetry-independent 20-atom ordered unit cell of CAN-CT was studied in detail to determine the total energy, κ_∞, F_{ij}, and $\overleftrightarrow{Z}^\star_i$. The results were then fit to Eqs. (6), etc. Only single-ion and pair terms of short distance were included in the cluster expansion. The number of terms kept in each fit was that necessary and sufficient to reproduce the results for the ordered cells. For simplicity, the force constants were not separated into short-range interactions and long-range dipole-dipole interactions in a self-consistent manner.[19].

Eqns. (1)-(2), with the parameters determined by the expansions (7), etc., can then be used to compute κ_s for any charge-neutral cation configuration ($\sum \sigma_i = 0$). The effect of cation ordering in CAN can be investigated as a special case of the full CAN-CT model with σ_i constrained to be +1 or -1. We simulated the order-disorder transition in CAN-CT by simulated sintering of 360-atom supercells at various temperatures, using a Metropolis

algorithm and Eq. (6) as the Hamiltonian. The order-disorder transition temperature was determined. For each given sintering temperature, various realizations of typical cation ordering were creating by "quenching" the instantaneous cation order at various times in the simulation. The average κ_s of these realizations were then computed.

The results are shown in Figure 1. The predicted dielectric constant increases as the simulated sintering temperature (and thus disorder) increases. Although no direct results for pure CAN are available, similar results are observed experimentally for analogous systems: when both ordered and disordered samples of the same composition are prepared, it is generally found that the disordered samples have κ_s about 10 % to 20 % greater than the ordered ones[20–22]

Simulations of CAN-CT as a function of x with fixed simulated sintering temperature slightly below the order-disorder transition temperature of CAN show a strong, nonlinear composition dependence of κ_s, in agreement with experiment[24] (see Figure 2).

IV. DISCUSSION

In all perovskites studied, the effective charges $Z^\star$ are anomalously large, especially $Z^\star_B$ and $Z^\star_{O,\|}$. Large $Z^\star$'s lead to large κ_s via Eq. (2). In simple perovskites, the same species s tends to have the same $Z^\star_s$ in different compounds (compare the titanates in Table I). However, two known processes can change $Z^\star_s$ significantly: (1) ferroelectric (FE) transitions (as in $BaTiO_3$ (BT) and $KNbO_3$ (KN)); (2) the inclusion of a second species on the perovskite B sublattice (such as occurs in CAN). Both processes lower the effective charges of the transition metal ion (Nb or Ti). Changes in $Z^\star_B$ and $Z^\star_{O,\|}$ reflect changes in the character of B-O bonding. Since $Z^\star_{Nb}$ is different in KN and CAN despite the fact that the Nb-O distances are very similar, one must conclude that B-O bonding in a perovskite depends strongly on the identity of cations on the surrounding B sites.

The large B and $O_\|$ effective charges in perovskites enhance the contribution of the Slater mode to the dielectric constant because B and O move against each other. In the ferroelectrics BT and KN, the softest mode in the cubic phase is Slater-like; however it

is unstable; the frequency associated with this mode is very temperature dependent, and thus the dielectric constant is strongly temperature-dependent (becoming very large at the FE transition temperatures). In the ground state of both systems, the two lowest modes are reversed. CT has remarkably different behavior (see Table II). The lowest frequency phonons of the cubic phase are Last-like (though strong mixing with a Slater-like mode occurs). There is a polar instability, but no ferroelectric transition occurs in CT: instead octahedral tilting transitions occur[23]. At low temperature, mode reversal of the other kind takes place: the Slater-like mode has the lowest frequency. In CAN, the Last-like mode is the lowest at all temperatures.

The differences between the lowest-frequency modes of the cubic phases are reasonable in light of the differences in tolerance factors. For BT and KN $t > 1$, and thus the B cations are "too small", and a Slater-type instability should exist. For CT and CAN, $t < 1$, and the A cations are "too small", therefore a Last-like instability should exist (although as noted, octahedral tilting transitions occur instead). The difference between CT and CAN in their low-temperature phases is more remarkable, and must be correlated with differences in the B-site chemistry.

V. CONCLUSIONS

First-principles computations have been used to compute the effective charges, phonon properties, and static dielectric constant κ_s of several perovskite-type compounds. The computed values for κ_s agree well with experiment. Differences between perovskites are related both to tolerance factor and to B site chemistry. A cluster expansion method was used to study κ_s in $(CaAl_{1/2}Nb_{1/2}O_3)_{1-x}$- $(CaTiO_3)_x$ as a function of composition and ordering. In CAN, κ_s was found to increase with disorder, and in CAN-CT, κ_s increased in a nonlinear manner with x, in agreement with experiment.

ACKNOWLEDGMENTS

I thank B.P. Burton, I. Levin, J. Petzelt, T. A. Vanderah, U. V. Waghmare, and V. Zelezny for useful discussions.

REFERENCES

[1] M. Born and K. Huang, "Dynamical Theory of Crystal Lattices" (Oxford: Oxford University Press), 1954.

[2] Ph. Ghosez, X. Gonze, and J.-P. Michenaud, Ferroelectrics **194**, 39 (1997).

[3] E. Cockayne and B. P. Burton, Phys. Rev. B **62**, 3735 (2000).

[4] S. Baroni, P. Giannozzi, and A. Testa, Phys. Rev. Lett. **58**, 1861 (1987).

[5] P. Giannozzi, S. de Gironcoli, P. Pavone and S. Baroni, Phys. Rev. B **43**, 7231 (1991).

[6] X. Gonze, D. C. Allan and M. P. Teter, Phys. Rev. Lett. **68**, 3603 (1992).

[7] G. Kresse and J. Hafner, Phys. Rev. B **47**, R558 (1993).

[8] G. Kresse, Thesis, Technische Universität Wien, 1993.

[9] G. Kresse and J. Furthmüller, Comput. Mat. Sci. **6**, 15 (1996).

[10] G. Kresse and J. Furthmüller, Phys. Rev. B **54**, 11169 (1996).

[11] E. Cockayne, J. Appl. Phys. **90**, 1459 (2001).

[12] D. Vanderbilt, Phys. Rev. B **41**, 7892 (1990).

[13] G. Kresse and J. Hafner, J. Phys.: Condens. Matter **6**, 8245 (1994).

[14] V. V. Lemanov, A. V. Sotnikov, E. P. Smirnova, M. Weihnacht, and R. Kunze, Solid State Comm. **110**, 611 (1999).

[15] W. J. Merz, Phys. Rev. **76**, 1221 (1949).

[16] W. Zhong, D. King-Smith and D. Vanderbilt, Phys. Rev. Lett. **72**, 3618 (1994).

[17] Ph. Ghosez, X. Gonze, Ph. Lambin, and J.-P. Michenaud, Phys. Rev. B **51**, 6765 (1995).

[18] C.-Z. Wang, R. Yu, and H. Krakauer, Phys. Rev. B **54**, 11161 (1996).

[19] X. Gonze, J.-C. Charlier, D. C. Allan, and M. P. Teter, Phys. Rev. B **50**, 13035 (1994).

[20] I. T. Kim, Y. H. Kim, and S. J. Chung, Jpn. J. Appl. Phys. part 1 **34**, 4096 (1995).

[21] R. J. Cava, J. J. Krajewski, and R. S. Roth, Mater. Res. Bull. **34** 355 (1999).

[22] I. Levin, J. Y. Chan, Geyer, Maslar, and Vanderah, J. Solid State Chem. **156**, 122 (2001).

[23] B. J. Kennedy, C. J. Howard, and B. C. Chakoumakos, J. Phys.: Condens. Matter **11**, 1479 (1999).

[24] I. Levin, J. Y. Chan, T. A. Vanderah, J. E. Maslar, and S. M. Bell, J. Appl. Phys. **90**, 904 (2001).

TABLE I: Comparative Born effective charges for different perovskites, as determined from first principles. When different crystal systems are given for the same compound, they represent "high" temperature and lowest temperature phases.

Compound	crystal system	$Z^\star_A$	$Z^\star_B$ ($Z^\star_{B'}$)		$Z^\star_{O,\parallel}$	$Z^\star_{O,\perp}$	Ref.
$CaTiO_3$	C	2.57	7.20		−5.69	−2.04	[3]
$CaTiO_3$	O	2.42	6.96		−5.38	−1.97	[3]
$SrTiO_3$	C	2.54	7.12		−5.66	−2.00	[16]
$BaTiO_3$	C	2.74	7.29		−5.75	−2.13	[2,17]
$BaTiO_3$	R	2.77	6.25		−5.05	−1.98	[2,17]
$PbTiO_3$	C	3.90	7.06		−5.83	−2.56	[16]
$PbTiO_3$	T	≈ 3.92	≈ 6.71		≈ −5.51	≈ −2.56	[16]
$BaZrO_3$	C	2.73	6.03		−4.74	−2.01	[16]
$KNbO_3$	C	1.12	9.67		−7.28	−1.74	[18]
$KNbO_3$	R	1.15	8.18		≈ −6.28	≈ −1.55	[18]
$CaAl_{1/2}Nb_{1/2}O_3$	C	2.59	3.97	6.37	−3.84	−1.96	this work
$CaAl_{1/2}Nb_{1/2}O_3$	M	2.45	4.01	6.25	−3.75	−1.94	[11]

TABLE II: Comparative phonon frequencies (in cm^{-1}) for different perovskites, as determined from first principles. Compound names and crystal system are abbreviated from Table I. For non-cubic systems, distinct frequencies are averaged into pseudotriplet frequencies. Imaginary frequency indicates instability. Modes are labelled as follows: ν_1: most similar to pure Last mode; ν_2: most similar to pure Slater mode; ν_3: O_6 bending; ν_4: B vs. B′.

Compound/ system	ν_1	ν_2	ν_3	(ν_4)	Ref.
CT/C	140 i	200	625		[3]
CT/O	217	98	509		[3]
BT/C	166	219 i	453		[2]
BT/R	163	220	474		[2]
KN/C	170	197 i	473		[18]
KN/R	172	216	534		[18]
CAN/C	48 i	304	733	487	[11]
CAN/M	194	302	613	425	[11]

TABLE III: Comparative κ_∞ and (pseudo)triplet contributions to κ_s for different perovskites, as determined from first principles. Experimental κ_s given, where known. Modes are ordered as in Table II.

Compund/system	κ_∞	κ_1	κ_2	κ_3	(κ_4)	κ_s	$(\kappa_s)_{\text{expt}}$ (T)
CT/O	6.1	7.2	260.0	1.4		274.7 [3]	331 (4 K) [14]
BT/R	5.1	15.7	35.6	0.6		57.0 [2]	
CAN/M	4.9	10.0	7.6	1.0	1.7	24.9 [11]	25.5 (298 K) [24]

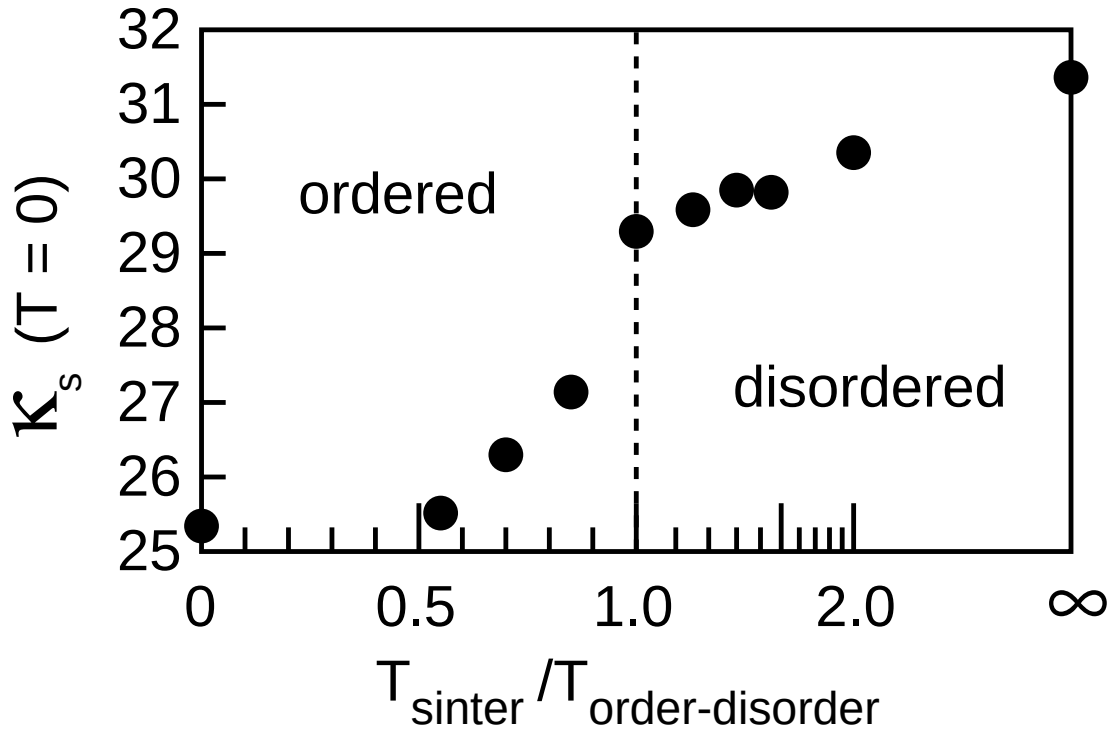

FIG. 1: Dielectric constant at T = 0 K vs. simulated sintering temperature in model for $CaAl_{1/2}Nb_{1/2}O_3$.

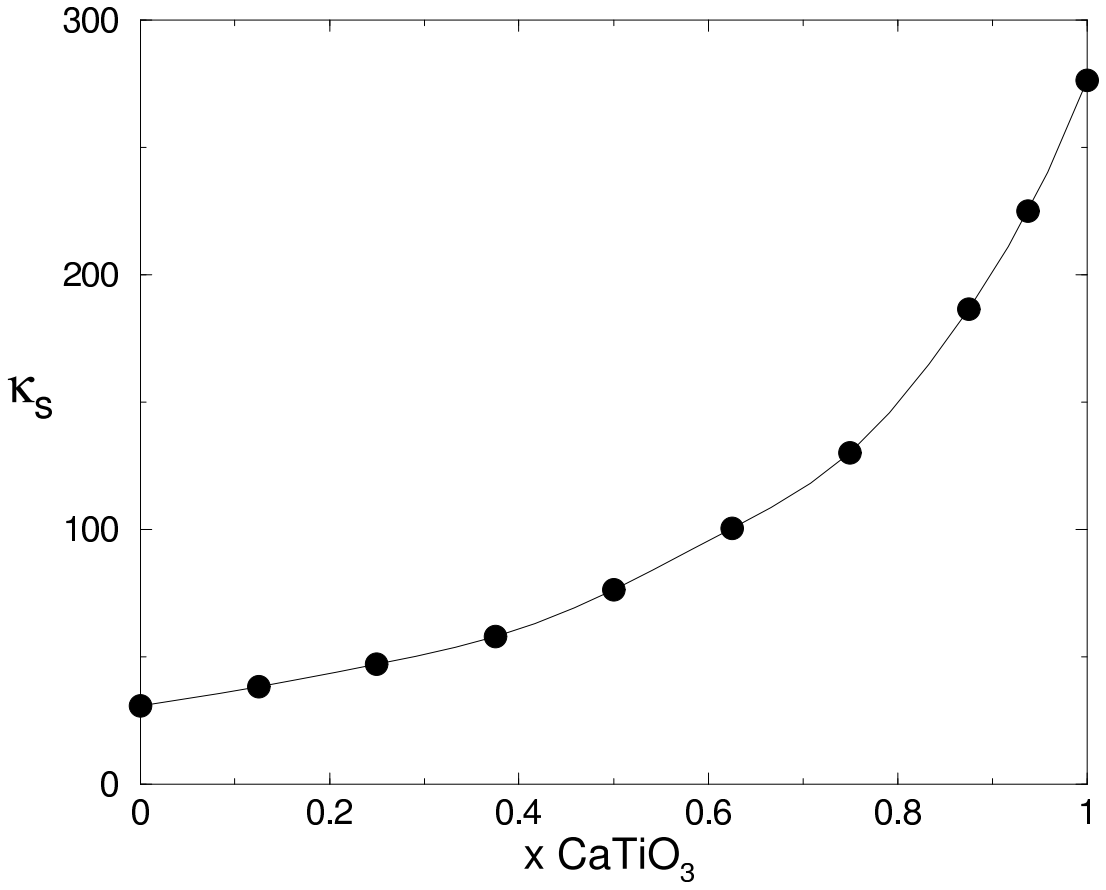

FIG. 2: Dielectric constant vs. composition x in model for $(CaAl_{1/2}Nb_{1/2}O_3)_{1-x}$- $(CaTiO_3)_x$.